

Effect of covalent antithrombin-heparin on activated protein C inactivation by protein C inhibitor

Received April 7, 2010; accepted June 6, 2010; published online June 10, 2010

Maria C. Van Walderveen, Leslie R. Berry and Anthony K.C. Chan*

Department of Pediatrics at McMaster University, David Braley Research Institute, Hamilton, Ontario, L8L 2X2, Canada

*Anthony K.C. Chan, Thrombosis & Atherosclerosis Research Institute (TaARI), David Braley Cardiac, Vascular and Stroke Research Institute (DBCVSRI), Hamilton General Hospital Campus, 237 Barton Street East, Hamilton, ON, L8L 2X2, Canada. Tel: +905 521 2100 (extn 73531), Fax: +905 577 1427, email: akchan@mcmaster.ca

Protein C in its activated form (APC) limits thrombin generation. Protein C inhibitor (PCI) readily neutralizes APC. Heparin accelerates this reaction, which may complicate anticoagulant treatment in patients with varying APC generation potential. A potent anticoagulant conjugate of antithrombin and heparin (ATH) was prepared, and its effect on APC+PCI reactions was tested. Second order rate constants for APC+PCI reactions were measured by discontinuous rate experiments in the presence of heparin or ATH. Similarly, low molecular weight fractions of heparin (LMWH) and ATH (LMWATH) were tested, as was high molecular weight ATH (HMWATH). Mechanisms of heparin or ATH binding to APC or PCI were assessed using electrophoresis. While heparin gave a higher maximal APC inhibition rate compared to ATH, peak inhibition rate was achieved at comparatively lower ATH concentrations. Since LMWH was ineffective at enhancing APC inhibition by PCI, unfractionated heparin likely acts by bridging APC and PCI. Unlike heparin, ATH may conformationally activate either APC or PCI since LMWATH significantly catalyses APC inhibition. Binding studies showed that ATH readily associates with APC. Thus, although a small fraction of ATH efficiently catalyses APC inhibition by PCI, complete ATH preparations induce a decreased maximal rate of APC-PCI formation compared to unfractionated heparin.

Keywords: Anticoagulant/antithrombin/heparin/protein C/protein C inhibitor.

Abbreviations: APC, activated protein C; ATH, covalent antithrombin-heparin; ECL, enhanced chemiluminescence; FVa, activated factor V; FVIIIa, activated factor VIII; H, heparin; HMWATH, high molecular weight ATH; IIa, thrombin; k_1 , pseudo-first order rate constant; k_2 , second order rate constant; LMWATH, low molecular weight ATH; PC, protein C; PCI, protein C inhibitor; serpin, serine protease inhibitor; TM, thrombomodulin; UFH, unfractionated heparin.

Thrombin (IIa), once bound to thrombomodulin (TM), forms a complex that readily cleaves protein C (PC) into activated PC (APC) (1, 2). APC functions as a potent anticoagulant by inactivating activated factors V (FVa) and VIII (FVIIIa) (3). Inactivation of FVa and FVIIIa prevents them from functioning within the tenase and prothrombinase complexes, and in turn reduces IIa generation (4–6). Natural inhibitors of APC are PC inhibitor (PCI), α -1-antitrypsin and α -2-macroglobulin, although, the latter two play more of a role after PCI is used up (7–9). PCI is a plasma glycoprotein involved in the regulation of coagulation, as well as fibrinolysis and reproduction (10–12). Within coagulation PCI, a member of the serine protease inhibitor (serpin) family, is capable of inhibiting a number of proteases (13, 14). PCI acts as a procoagulant through its inhibition of APC. The PC pathway plays a key role within coagulation. It is important to look at the inhibitors of the PC pathway. Also, it is significant to determine the effects that anticoagulants have on these PC pathway inhibitors. PCI inhibition of APC is enhanced in the presence of heparin (H) (7, 10, 15). The current study was done to determine the effect(s) of a novel covalent antithrombin–heparin (ATH) anticoagulant on APC inhibition by PCI.

Chan *et al.* (16) developed an ATH complex to overcome several limitations found for H. Structurally, the covalent linkage of H to AT is a result of a Schiff base formation followed by an Amadori rearrangement (16). The formation of a stable keto-amine linkage of H to AT occurs primarily at the N-terminal amino acid, and only a small portion at Lys139, of AT (17). AT forms a 1 : 1 ratio with H, where all ATH H chains contain a high affinity pentasaccharide sequence. On average the H chains of ATH are longer, compared to unfractionated H (UFH), with an average molecular weight of 18 kDa (16). Given the unusual and desirable properties of H selection that occurs during the formation of ATH, it is important to study ATH's effects on APC+PCI compared to UFH. The ATH complex, compared to H, has been shown to have a longer half-life, reduced non-specific plasma protein and endothelial cell binding, and increased inhibition of IIa (16, 18, 19). Moreover, ATH indicated promising results for surface coating. *In vivo* studies in rabbits showed that insertion of catheters coated with ATH had reduced fibrin accretion and thrombus formation, compared to H (20–22). Moreover, injection of ATH subcutaneously and intratracheally showed its localization and compartmentalization to the site of injection (16). ATH, thus, may prove beneficial for the treatment of respiratory distress syndrome, which is

characterized by interstitial and intra-alveolar IIa generation and fibrin deposition (23–26). To continue to define ATH function within the PC pathway, the present study will investigate effects of ATH on APC inhibition by PCI, and the mechanism of this interaction.

Materials and Methods

Materials

All reagents used were of analytical grade. Polybrene and Alcian Blue 8 GX were both obtained from Sigma (Mississauga, ON, USA). UFH, from porcine intestinal mucosa, was obtained from Sigma (St Louis, MO, USA). Lovenox (enoxaparin sodium), a low molecular weight H (LMWH), was purchased from Sanofi Aventis. The LMWH was obtained by the depolymerization of native UFH from the porcine intestinal mucosa by base elimination (27). The molecular weight ranges from 3800–5000 Da, with the average being 4500 Da (27). Thus, the LMWH contains ~11–16 monosaccharide residues. APC came from Enzyme Research Laboratories (South Bend, IN, USA). The substrate S-2366 (L-pyroglyutamyl-L-prolyl-L-arginine-p-nitroaniline hydrochloride) was purchased from Diapharma (West Chester, OH, USA). Dr Stenflo from Lund University, University Hospital (Malmö, Sweden) kindly provided the PCI. ATH was prepared as described earlier (16).

Preparation of low molecular weight ATH and high molecular weight ATH

High molecular weight ATH (HMWATH) and low molecular weight ATH (LMWATH) were prepared by repeated gel filtration as described by Paredes *et al.* (28). In brief, fractionation of ATH by molecular weight was done using a Sephadex G-200 column. The first 2–9% of the fractions collected was the HMWATH (with H chains containing >83 saccharide units), and the latter 30% of fractions were taken as LMWATH. Two LMWATH fractions were investigated. A very short chain containing LMWATH (designated LMWATH 1) was obtained by pooling the last 2–9% of the gel filtered ATH fractions, making it a molecule containing an H chain of ≤10 saccharide units in size. A somewhat larger LMWATH (designated LMWATH 2) was prepared from a pool of the last 16–25% of fractions from the gel filtered ATH. This pool has molecules with H chains ranging in size from 13–19 saccharide units, with an average size of 16 saccharide residues. Freeze-dried pools were re-suspended in H₂O and dialysed against 0.016 M Na₂HPO₄, 0.004 M NaH₂PO₄ and 0.15 M NaCl (PBS) buffer.

Second order rate constant inhibition assay of APC by PCI in the presence or absence of UFH, LMWH, ATH, HMWATH or LMWATH

The method for catalysis by UFH, LWMH, ATH, HMWATH or LMWATH of APC inhibition by PCI is derived and modified from Neese *et al.* (1998) (29) and Friedrich *et al.* (2001) (30). Discontinuous second order rate constant inhibition assays were performed. APC was inhibited by PCI under pseudo-first order conditions at 37°C. The same 20 mM Tris-HCl, 0.10 M NaCl and 0.1% bovine serum albumin (TS-BSA) buffer, as used by Friedrich *et al.* (30) but with added 2.5 mM CaCl₂ was used for the kinetic experiments. Briefly, in six wells of a 96-well flat-bottom microtitre plate, 10 µl of APC [6.6 nM] was added. In well six 10 µl TS-BSA buffer was added. In wells one through five at various time intervals (at anywhere from 3 to 240 s intervals) 10 µl of the PCI [60 nM] in the presence or absence of UFH, LWMH, ATH, HMWATH or LMWATH [6–600 nM for all catalysts] was added. The reaction was terminated by the addition of 2.0 mg/ml polybrene, and in the presence of S-2366 the chromogenic substrate specific for APC. Residual enzyme activity was visualized using a SpectraMax Plus 384 plate reader at 405 nm. The pseudo-first order rate constant (k_1) was calculated as the negative slope from the plot $\ln(V_t/V_0)$, where V_t is the final remaining enzyme activity at time t and V_0 is the initial enzyme activity, versus inhibition time. The second order rate constant (k_2) was calculated by dividing k_1 by the concentration of the inhibitor.

Electrophoresis and western blot analysis of complexes with APC or PCI

A native polyacrylamide gel (7.5% separating gel) was run to determine APC and PCI interaction with AT, UFH or ATH. Loads on the gels were 5 µg of either APC or PCI in the presence of 10 µg of AT, 2.5 µg of UFH or 10 µg of ATH. Controls included 5 µg of APC alone, 5 µg of PCI alone, APC+PCI (5 µg of each), 10 µg of AT alone, 10 µg of ATH alone and 2.5 µg of UFH alone. Incubations of APC or PCI with AT, UFH or ATH were for 1 h at 37°C, as was that for APC with PCI. Once the gel was run, using a running buffer containing sodium dodecyl sulphate (SDS), it was stained using the ProteoSilver™ Silver Stain Kit (Sigma, St Louis, MO, USA) to detect protein-containing bands. A third gel was run under the same conditions and containing the following samples: (i) 10 µg of AT alone; (ii) 0.05 µg APC alone; (iii) 10 µg of AT + 0.05 µg APC; (iv) 10 µg of AT + 0.05 µg APC + 2.5 µg of UFH; and (v) 2.5 µg of UFH alone. The samples were electrophoretically transferred to a polyvinylidene fluoride (PVDF) membrane. The membrane was probed with a primary sheep anti-human PC affinity-purified IgG antibody (4.0×10^{-4} mg/ml). This was followed with a donkey anti-sheep IgG peroxidase conjugate secondary antibody (1.1×10^{-4} mg/ml). Detection of the bands was through the use of enhanced chemiluminescence (ECL) Plus Western Blotting Detection Kit from GE Healthcare (Piscataway, NJ, USA). The bands were visualized using the Typhoon 9410 (GE Healthcare, Baie d'Urfe, QC, USA).

Results

APC inhibition by PCI catalysed by UFH, LMWH, ATH, LMWATH and HMWATH

Discontinuous second order rate constant inhibition assays demonstrated that UFH increased APC inhibition by PCI to a significantly greater extent compared to ATH (Fig. 1A). At peak values, UFH ($k_2 = 3.0 \times 10^7 \pm 2.0 \times 10^6$) was a much more effective catalyst compared to ATH ($k_2 = 2.0 \times 10^7 \pm 1.2 \times 10^6$; $P = 0.005$). Also, the peak k_2 value of UFH was observed at a higher catalyst concentration compared to ATH (300 nM versus 60 nM, respectively). The plot of k_2 versus varying UFH concentrations produced a bell-shaped curve (Fig. 1A). Although there was a small peak present for ATH, higher concentrations resulted in a plateau effect. Compared to UFH, LMWH significantly reduced the rate of APC inhibition by PCI ($P < 0.001$; Fig. 1A). LMWATH 1, that possessed a very short H chain, produced similar results to those for LMWH. However, LMWATH 2 and HMWATH were more effective at catalysing APC inhibition by PCI compared to ATH (Fig. 1B). Control experiments of APC inhibition by AT alone, and thus in the absence of PCI, resulted in a very slow rate of inhibition ($k_2 < 3.1 \times 10^3 \pm 3.2 \times 10^2 \text{ M}^{-1} \text{ min}^{-1}$; $n = 3$). The addition of UFH slightly enhanced the rate of inhibition to $k_2 < 4.7 \times 10^3 \pm 1.2 \times 10^3 \text{ M}^{-1} \text{ min}^{-1}$ ($n = 3$). The rate of inhibition of APC by ATH was further enhanced to $k_2 = 1.4 \times 10^4 \pm 1.1 \times 10^3 \text{ M}^{-1} \text{ min}^{-1}$ ($n = 3$).

ATH or UFH binding to APC or PCI

A gel formed under native conditions (pH = 8.8), however using SDS in the running buffer to prevent non-selective weak interactions with the gel matrix, was run to evaluate binding of UFH and ATH to APC and PCI. Using these conditions there seemed to be little to no binding of UFH to APC or PCI (Fig. 2). Similarly, ATH did not readily bind to PCI (Fig. 2). However, ATH did form a complex with the

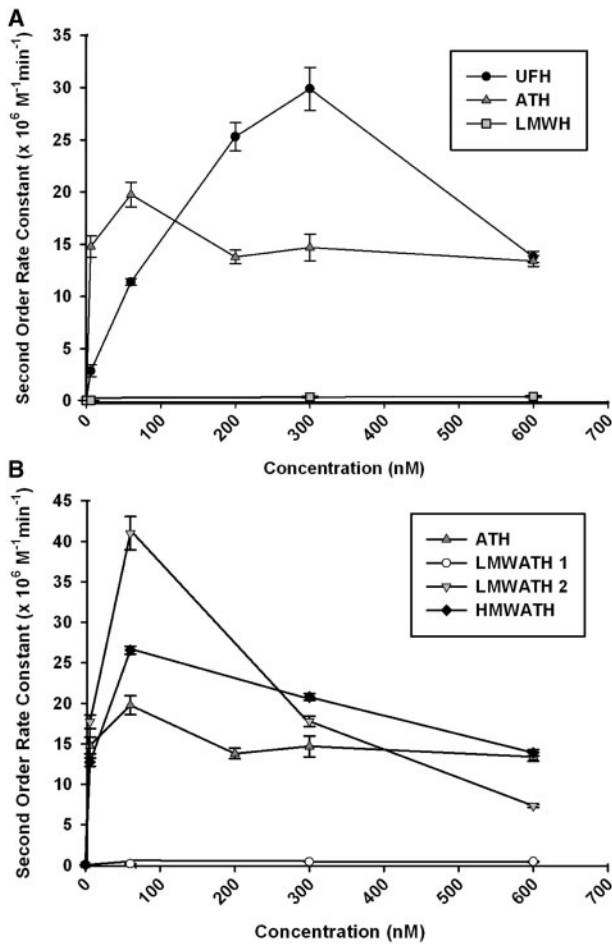


Fig. 1 Catalysis of APC inhibition by PCI. The rate of APC [6.6 nM] inhibition by PCI [60 nM] was determined in the presence of (A) UFH, ATH or LMWH; (B) ATH, LMWATH 1, LMWATH 2 or HMWATH. During gel filtrations of ATH ('Materials and Methods'), LMWATH 1 was prepared from the last 2–9% of fractions and LMWATH 2 was prepared from the last 16–25% of fractions. Concentrations of each of these catalysts ranged from 0–600 nM.

APC, as indicated by the appearance of the dark high molecular weight band in lane 6 of Fig. 2A, not visible in lanes with ATH or APC alone. Using the same conditions, control experiments looking at AT binding to APC or PCI, showed only slight interaction of AT with APC, as seen by a faintly visible band in lane 4 of Fig. 3A. The presence of UFH potentially enhanced this reaction (Fig. 3A, lane 5). No complex formation is found for AT with PCI in the presence or absence of UFH (Fig. 3B). Western blot analysis was done to further confirm these findings. As seen in Fig. 4 (lane 3) the addition of APC with AT produces a long smear, compared to APC alone. Upon the addition of UFH (lane 4) there is a discrete band formed by APC interaction with AT.

Discussion

PCI inhibits APC slowly ($k_2 = 2.0 \times 10^5 \text{ M}^{-1} \text{ min}^{-1}$) in comparison to other serpins (10, 31). Consistent with previous studies (7, 10, 15), the present work shows that H enhances this rate of inhibition significantly ($k_2 = 3.0 \times 10^7 \text{ M}^{-1} \text{ min}^{-1}$). From the current study we find that like UFH, ATH can catalyze APC inhibition by PCI.

H functions through template-mediated inactivation, where H binds both APC and PCI, bridging the two molecules to enhance their interaction (32). The bell-shaped curve produced when plotting UFH concentration versus k_2 , as seen in Fig. 1A, is characteristic of a template-mediated mechanism. The reduced rate of APC inhibition by PCI in the presence of LMWH further supports this mechanism. Thus, the efficient catalysis of APC inhibition by PCI is likely dependent on H chain length. Although APC inhibition by PCI, in the presence of H, works mainly through the template-mediated mechanism, small H molecules may still assist PCI reactivity with APC (33). There is no strong threshold for H oligosaccharide size

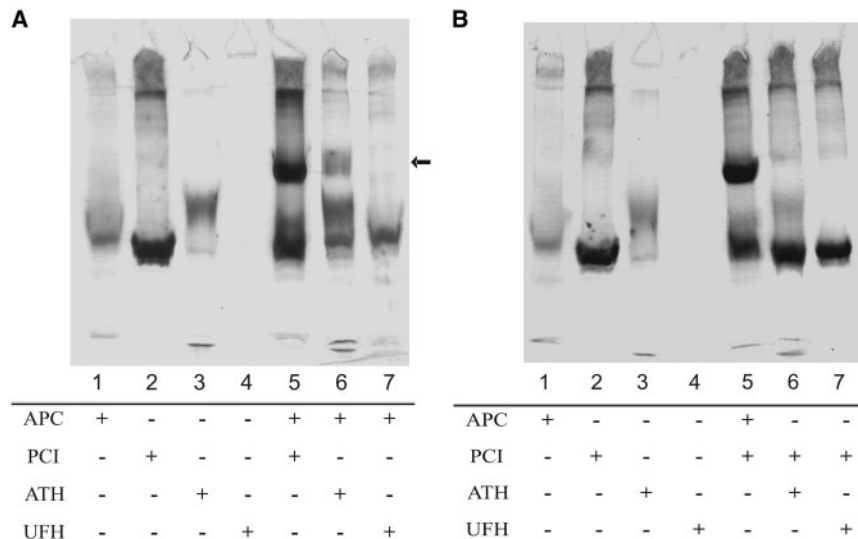


Fig. 2 Electrophoresis of APC (A) or PCI (B) in the presence and absence of UFH or ATH. Lanes 1–4 contain APC [5 µg], PCI [5 µg], ATH [10 µg] and UFH [2.5 µg] alone, respectively. Lane 5 contains both APC [5 µg] and PCI [5 µg]. Lanes 6 and 7 contains APC [5 µg] (A) or PCI [5 µg] (B) in the presence of ATH [10 µg] or UFH [2.5 µg], respectively. Proteins were visualized using a ProteoSilver™ Silver Stain Kit (Sigma).

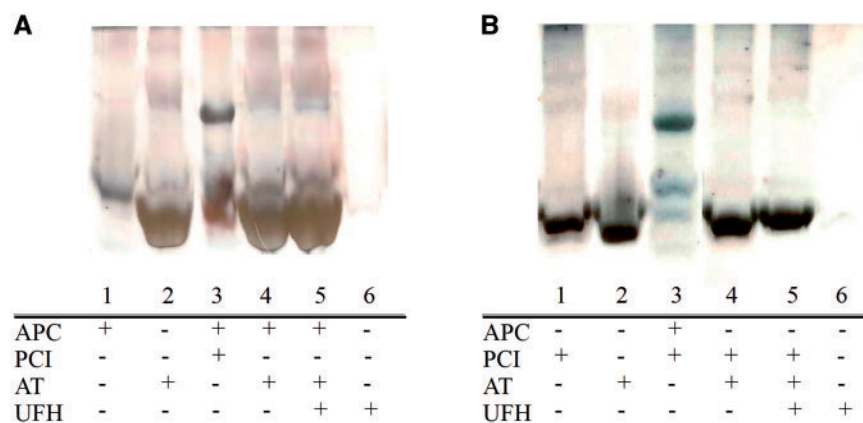


Fig. 3 Electrophoresis of APC (A) or PCI (B) in the presence and absence of AT. Lanes 1, 2 and 6 contain APC [5 µg] or PCI [5 µg], AT [10 µg] and UFH [2.5 µg] alone, respectively. Lane 3 contains both APC [5 µg] and PCI [5 µg]. Lanes 4 and 5 contain APC [5 µg] (A) or PCI [5 µg] (B) in the presence of AT [10 µg] or AT [10 µg] + UFH [2.5 µg], respectively. Proteins were visualized using a ProteoSilver™ Silver Stain Kit (Sigma).

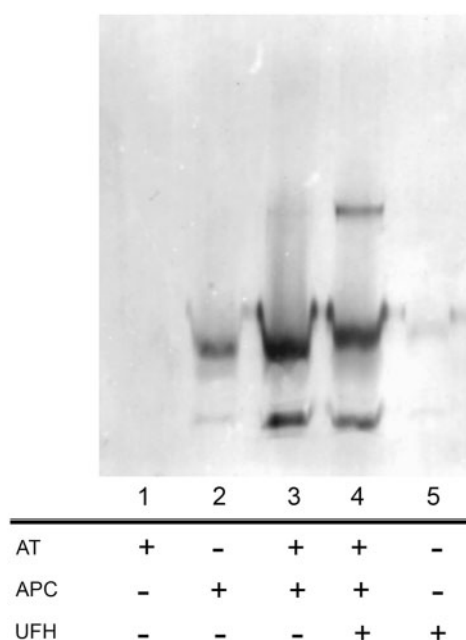


Fig. 4 Western blot analysis of APC complex formation with AT in the presence and absence of UFH. As controls, lanes 1, 2 and 5 contain AT [10 µg], APC [0.05 µg] and UFH [2.5 µg] alone, respectively. Lane 3 contains AT [10 µg] and APC [0.05 µg]. Similar to lane 3, lane 4 contains the AT and APC, but in the presence of UFH [2.5 µg]. After probing with anti-PC primary and anti-IgG-peroxidase secondary antibodies, protein bands were visualized using an ECL Plus Detection Kit (GE Healthcare).

dependence for increased APC inhibition (33), hence the broadness to the curve in Fig. 1A. Also, from Fig. 1A, it becomes evident that the curve for ATH does not reflect a template-mediated effect. Although there is a small peak, the main mechanism by which ATH functions is likely through conformational activation. We speculate that ATH causes a conformational change in APC, resulting in an increased interaction with PCI. Moreover, ATH may bind to APC in such a way that the H moiety does not bridge APC with PCI. Although the majority of ATH may be unable to bridge APC to PCI, a small peak suggests some minor template-mediated inactivation may occur, which might be representative of a small

sub-population of ATH containing longer H chains (16, 28). We speculate that these ATH molecules, once bound to APC, may potentially assist interaction with PCI.

To further understand the mechanism by which ATH functions, discontinuous second order rate constant inhibition assays measuring APC inhibition by PCI were performed in the presence of either of two LMWATHs, or a HMWATH (Fig. 1B). The HMWATH and LMWATH 2 (the LMWATH with the longer H chain) both presented a higher rate of catalysis, compared to ATH. From this we can conclude that there is no strong H oligosaccharide size dependence for the catalysis of APC inhibition by PCI. The increased effective catalytic function of LMWATH 2, compared to ATH, may suggest that LMWATH 2 is capable of interacting with APC and PCI in an unusual configuration where AT is activating APC and the length of H is optimal for binding to PCI. Unlike LMWATH 2, LMWATH 1 resulted in a significantly lower catalytic function. The rate of APC inhibition by PCI is only ~10-fold faster if LMWATH 1 is present, compared to APC inhibition by PCI alone (Fig. 1B). AT alone does not affect APC inhibition by PCI. The rate of inhibition of APC by AT is very slow (in the absence of PCI). Similarly the AT moiety of ATH does not readily inhibit APC itself in the absence of PCI. The rate for direct inhibition by ATH was more than a thousand fold lower than that found for APC inhibition by PCI+ATH. Together from these findings we conclude that the H chain of ATH has to be long enough for the GAG to interact with APC and/or PCI to stabilize or orientate the complex properly and allow for optimal catalysis of the reaction between APC and PCI.

To evaluate the interaction of UFH or ATH with APC or PCI, gel electrophoresis was performed. Having the pH environment at 8.8, as found in the non-denaturing gels (Fig. 2), resulted in sustained binding of only ATH to APC. H is a highly negatively charged molecule that readily binds to the positively charged amino groups (e.g. lysyl and arginyl amino groups). H interacts with APC through Lys37-39 (37-loop) (32). It is also known that H interacts with

PCI through Lys266, Arg269, Lys270 and Lys273, which are part of the H-helix (10). Elevation of pH results in the increased deprotonation of these lysyl amino groups causing a loss of positive charge. Consequently, H is no longer able to bind through these charge attractions to either APC or PCI. However, ATH is still capable of binding APC, suggesting that the AT moiety of ATH may be interacting with the enzyme. These results, together with findings illustrated in Fig. 1, show that ATH may in fact function through conformational APC activation mediated by AT. The difference in the mechanism of inhibition between ATH and UFH, is a consequence of the presence of the AT moiety in ATH. From the gels seen in Fig. 3, only some slight interaction of AT with APC was observed. Western blot analysis indicated that APC does interact with AT, and this binding was enhanced by the addition of UFH (Fig. 4). APC combined with AT (as seen in lane 3) runs as a smear, indicating slight affinity between the two molecules. Unlike the gel shown in Fig. 3, a necessarily lower ratio of APC to AT was used for the western blots to avoid over exposure. Even at these low APC concentrations (0.05 μg) there is evidence of interaction between APC and AT. UFH enhances this reaction significantly, and the discrete band seen in lane 4 (Fig. 4) indicates a tight affinity of AT to APC. The covalent linkage of H to AT, thus, affects the orientation and interaction by which the AT complexes with the APC. Future experiments with products formed by a progressive removal of the H from ATH by heparinase, prior to interaction with APC and PCI, could provide further insight into the role of the AT moiety in ATH.

In conclusion, studies have shown ATH to be a potent anticoagulant (16). ATH is capable of catalysing the rate of inhibition for a number of coagulation factors that affect PC activation and IIa generation (16, 34, 35). The present investigation further defines the function of ATH within the coagulation cascade. The reduced APC inhibition by PCI in the presence of ATH, compared to UFH, results in persistence of APC within the vascular system. Consequently, APC is left to act on FVa and FVIIIa, leading to an ultimate reduction in IIa generation. Through the course of this work, it became evident that ATH functions through a very different mechanism compared to UFH in catalysing APC inhibition by PCI. ATH operates largely through conformationally activating APC, whereas UFH functions by bridging the APC and PCI. Overall, these results add to our understanding of the mechanisms of ATH function. This will allow further development of ATH as a novel treatment for thrombotic conditions.

Acknowledgements

We greatly appreciate the generous gift of PCI from Dr Johan Stenflo.

Funding

Grant-in-Aid from the Heart and Stroke Foundation of Ontario (NA6423). A.K.C. Chan is supported by the Bayer Thrombosis and Hemostasis Research Grant.

Conflict of interest

None declared.

References

1. Koeppel, J.R., Seitova, A., Mather, T., and Komives, E.A. (2005) Thrombomodulin tightens the thrombin active site loops to promote protein C activation. *Biochemistry* **44**, 14784–14791
2. Bourin, M. and Lindahl, U. (1993) Glycosaminoglycans and the regulation of blood coagulation. *Biochem. J.* **289**, 313–330
3. Kalafatis, M., Rand, M.D., and Mann, K. (1994) The mechanism of inactivation of human factor V and human factor Va by activated protein C. *J. Biol. Chem.* **269**, 31869–31880
4. Spencer, F.A. and Becker, R.C. (1997) The prothrombinase complex: assembly and function. *J. Thromb. Thrombolysis* **4**, 357–364
5. Nesheim, M., Taswell, J., and Mann, K. (1979) The contribution of bovine factor V and factor Va to the activity of prothrombinase. *J. Biol. Chem.* **254**, 10952–10962
6. Davie, E.W., Fujikawa, K., and Kiesel, W. (1991) The coagulation cascade: initiation, maintenance, and regulation. *J. Biochem.* **30**, 10363–10368
7. Suzuki, K., Nishioka, J., Kusumoto, H., and Hashimoto, S. (1984) Mechanism of inhibition of activated protein C and protein C inhibitor. *J. Biochem.* **95**, 187–195
8. Hoogendoorn, H., Toh, C., Nesheim, M., and Giles, A. (1991) Alpha-2-Macroglobulin binds and inhibits activated protein C. *Blood* **78**, 2283–2290
9. Heeb, M.J. and Griffin, J.H. (1988) Physiologic inhibition of human activated protein C by α_1 -antitrypsin. *J. Biol. Chem.* **263**, 11613–11616
10. Suzuki, K. (2000) Protein C inhibitor (PAI-3): structure and multi-function. *Fibrinolysis Proteol.* **14**, 133–145
11. Hermans, J.M., Jones, R., and Stone, S.R. (1994) Rapid inhibition of the sperm protease acrosin by protein C inhibitor. *Biochemistry* **33**, 5440–5444
12. Mushunje, A., Evans, G., Brennan, S.O., Carrell, R.W., and Zhou, A. (2004) Latent antithrombin and its detection, formation and turnover in the circulation. *J. Thromb. Haemost.* **2**, 2170–2177
13. Geiger, M., Zechmeister-Machhart, M., Uhrin, P., Hufnagl, P., Ecker, S., Priglinger, U., Jianjun, X., Xinglong, Z., and Binder, B. (1996) Protein C inhibitor (PCI). *Immunopharmacology* **32**, 53–56
14. Huntington, J., Kjellberg, M., and Stenflo, J. (2006) Crystal structure of protein C inhibitor provides insight into hormone binding and heparin activation. *Structure* **11**, 205–215
15. Pratt, C.W. and Church, F.C. (1992) Heparin binding to protein C inhibitor. *J. Biol. Chem.* **267**, 8789–8794
16. Chan, A., Berry, L., O'Brodovich, H., Klement, P., Mitchell, L., Baranowski, B., Monagle, P., and Andrew, M. (1997) Covalent antithrombin-heparin complex with high anticoagulant activity: intravenous, subcutaneous and intratracheal administration. *J. Biol. Chem.* **272**, 22111–22117
17. Mewhort-Buist, T., Junop, M., Berry, L., Chindemi, P., and Chan, A. (2006) Structural effects of a covalent linkage between antithrombin and heparin: covalent N-terminus attachment of heparin enhances the maintenance of antithrombin's activated state. *J. Biochem.* **140**, 175–184
18. Chan, A., Paredes, N., Thong, B., Chindemi, P., Paes, B., Berry, L., and Monagle, P. (2004) Binding of heparin to plasma proteins and endothelial surfaces is inhibited by

- covalent linkage to antithrombin. *Thromb. Haemost.* **91**, 1009–1018
19. Berry, L., Stafford, A., Fredenburgh, J., O'Brodovich, H., Mitchell, L., Weitz, J., Andrew, M., and Chan, A. (1998) Investigation of the anticoagulant mechanisms of a covalent antithrombin-heparin complex. *J. Biol. Chem.* **273**, 34730–34735
 20. Klement, P., Du, Y.J., Berry, L., Andrew, M., and Chan, A. (2002) Blood-compatible biomaterials by surface coating with a novel antithrombin-heparin covalent complex. *Biomaterials* **23**, 527–535
 21. Du, Y.J., Klement, P., Berry, L., Tressel, P., and Chan, A. (2005) *In vivo* rabbit acute model tests of polyurethane catheters coated with a novel antithrombin heparin covalent complex. *Thromb. Haemost.* **94**, 366–372
 22. Klement, P., Du, Y.J., Berry, L., Tressel, P., and Chan, A. (2006) Chronic performance of polyurethane catheters covalently coated with ATH complex: a rabbit jugular vein model. *Biomaterials* **27**, 5107–5117
 23. Berry, L., Klement, P., Andrew, M., and Chan, A. (2003) Effect of covalent serpin-heparinoid complexes on plasma thrombin generation of fetal distal lung epithelium. *Am. J. Respir. Cell Mol. Biol.* **28**, 150–158
 24. Brus, F., van Oeveren, W., Heikamp, A., Okken, A., and Oetomo, S. (1996) Leakage of protein into lungs of preterm ventilated rabbits is correlated with activation of clotting, complement, and polymorphonuclear leukocytes in plasma. *Pediatr. Res.* **39**, 958–965
 25. Bachofen, M. and Weibel, E.R. (1982) Structural alterations of lung parenchyma in adult respiratory distress syndrome. *Clin. Chest Med.* **3**, 35–56
 26. Gajl-Peczalska, K. (1964) Plasma protein composition of hyaline membrane in the newborn as studies by immunofluorescence. *Arch. Dis. Child.* **39**, 226–231
 27. Sanofi Aventis. (2007) Lovenox: enoxaparin sodium injection. *Product information sheet*, 1–2
 28. Paredes, N., Wang, A., Berry, L., Smith, L., Stafford, A., Weitz, J., and Chan, A. (2003) Mechanisms responsible for catalysis of the inhibition of factor Xa or thrombin by antithrombin using covalent antithrombin-heparin complexes. *J. Biol. Chem.* **278**, 23398–23409
 29. Neese, L., Wolfe, C., and Chruch, F. (1998) Contribution of basic residues of the D and H-helices in heparin binding to protein C inhibitor. *Arch. Biochem. Biophys.* **355**, 101–108
 30. Friedrich, U., Blom, A., Dahlback, B., and Villoutreix, B. (2001) Structural and energetic characteristics of the heparin-binding site in antithrombotic protein C. *J. Biol. Chem.* **276**, 24122–24128
 31. Hermans, J.M. and Stone, S.R. (1993) Interaction of activated protein C with serpins. *Biochem. J.* **295**, 239–245
 32. Glasscock, L.N., Gerlitz, B., Cooper, S., Grinnell, B., and Church, F.C. (2003) Basic residues in the 37-loop of activated protein C modulate inhibition by protein C inhibitor but not by alpha-1-antitrypsin. *Biochim. Biophys. Acta* **1694**, 106–117
 33. Pratt, C.W., Whinna, H.C., and Church, F.C. (1992) A comparison of three heparin-binding serine proteinase inhibitors. *J. Biol. Chem.* **267**, 8795–8801
 34. Patel, S., Berry, L., and Chan, A. (2007) Analysis of inhibition rate enhancement by covalent linkage of antithrombin to heparin as a potential predictor of reaction mechanism. *J. Biochem.* **141**, 25–35
 35. Berry, L., Becker, D.L., and Chan, A. (2002) Inhibition of fibrin-bound thrombin by a covalent antithrombin-heparin complex. *J. Biochem.* **132**, 167–176